

Intermolecular interactions of extended aromatic ligands: the synchrotron molecular structures of $[\text{Ru}(\text{bpy})_2(\text{N-HSB})].2\text{PF}_6$ and $[\text{Ru}(\text{bpy})_2(\text{N-}\frac{1}{2}\text{HSB})].2\text{PF}_6$

Daniel J. Gregg, Christopher M. Fitchett and Sylvia M. Draper*

Received (in Cambridge, UK) 21st March 2006, Accepted 30th May 2006

First published as an Advance Article on the web 16th June 2006

DOI: 10.1039/b604131k

An off-set stack and a saddle-like distortion are revealed by the molecular structures of $[\text{Ru}(\text{bpy})_2(\text{N-HSB})].2\text{PF}_6$ and $[\text{Ru}(\text{bpy})_2(\text{N-}\frac{1}{2}\text{HSB})].2\text{PF}_6$.

The processes by which molecular systems undergo aggregation have received much attention because they are key to the delivery of pre-determined supramolecular structures at the molecular design stage. The intermolecular forces known to have an overriding effect on molecular aggregation include hydrogen-bonding,¹ solvent,² charge-charge³ and π -stacking interactions.⁴ Molecular families where the latter are significant include the large planar aromatics such as the hexabenzocoronenes.⁵ Remarkable differences in the aggregation of these systems due to changes in peripheral organic substituents have been observed,⁶ but the influence and inclusion of metal connectors is far rarer. In two emergent molecular families, the eilatins and the nitrogen-heterosuperbenzenes (N-HSBs),⁷ extended fused aromatic rings and proven ligand function allow particular attention to be given to the resulting transition metal coordination complexes.

The successful syntheses and structural elucidation of Ru(II)-eilatin,⁸ -isoeilatin⁹ and -dibenzoilatin coordinated compounds gives some indication of the nature of their π -stacking. The solid-state structure of the latter shows a prevalence for strong dimeric π -stacking interactions, despite a slight out-of-plane bowing of the aromatic platform.¹⁰ In this context the spectroscopic characterization of $[\text{Ru}(\text{bpy})_2(\text{N-HSB})].2\text{PF}_6$ (**1**)¹¹ and $[\text{Ru}(\text{bpy})_2(\text{N-}\frac{1}{2}\text{HSB})].2\text{PF}_6$ (**2**)¹² (where bpy = 2,2'-bipyridine, see Fig. 1) provided a welcome addition to on-going investigations into large-surface ligands, and demonstrated the aggregation of **1** but not **2** in dilute solutions. Two assumptions were made; firstly, that the out-of-plane twisting of the free phenyls in N- $\frac{1}{2}$ HSB prevented the aggregation of **2**, and secondly that a dimeric aggregate of **1** was most likely. The effect of the increase in conjugation of **1** compared to eilatin (13 and 7 fused aromatic rings, respectively) in terms of enhanced aggregation or in the bowing or distortion of the aromatic plane of **2** could not be made in the absence of structural data. Such twisted distortion of the aromatic manifold of hexabenzocoronenes¹³ and fused polyaromatic hydrocarbons¹⁴ has previously been observed.

In this current work we report the first molecular structures of the complexes $[\text{Ru}(\text{bpy})_2(\text{N-HSB})].2\text{PF}_6$ (**1**)[†] and $[\text{Ru}(\text{bpy})_2(\text{N-}\frac{1}{2}\text{HSB})].2\text{PF}_6$ (**2**)[‡] which allow a detailed consideration of both their molecular structure and solid-state packing. Vapour

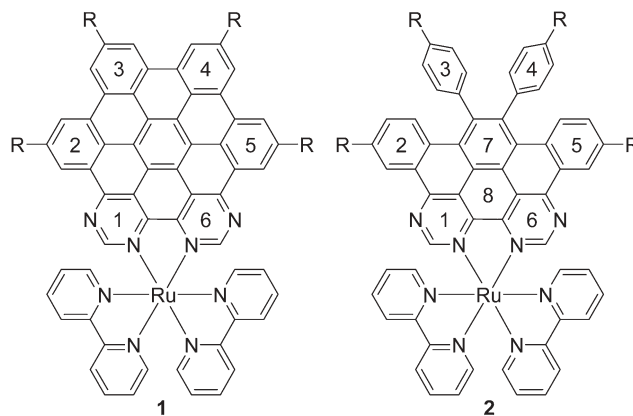


Fig. 1 Complexes $[\text{Ru}(\text{bpy})_2(\text{N-HSB})].2\text{PF}_6$ (**1**) and $[\text{Ru}(\text{bpy})_2(\text{N-}\frac{1}{2}\text{HSB})].2\text{PF}_6$ (**2**) showing the ring labelling for N-HSB and N- $\frac{1}{2}$ HSB ligands. R = *tert*-butyl.

diffusion of ether into acetonitrile solutions of each complex yielded crystals which were too small and weakly diffracting for standard X-ray diffraction techniques. In the alternative these were submitted to the synchrotron source at SRS Daresbury.¹⁵ The molecular structures confirm that both **1** and **2** are mononuclear, with the bidentate N-HSB or N- $\frac{1}{2}$ HSB contributing to the octahedral geometry about the ruthenium metal centre (see Table 1). Dramatic structural differences arise however, both in the planarity of the ring-fused portion of the ligands and in the nature of the intermolecular interactions. These are primarily a consequence of the size of the aromatic platform and in turn the orientation of the non-planar (labeled 3 and 4 in Fig. 1).

N-HSB comprises 13 fused rings. As a ligand its aromaticity is reflected in the solid-state by the delocalisation of its CC bonds (average C–C bond length 1.39(2) Å) and in the high degree of planarity (mean deviation 0.08 Å) observed in **1**. This results in significant π - σ face-to-face stacking interactions that extend beyond simply dimeric and that verify the observation of solution aggregation in both the spectroscopic and electrochemical data.

Two stacking interactions, eclipsed and staggered, are apparent for each N-HSB ligand and these combine to give a unique off-set

Table 1 Ruthenium–nitrogen distances (Å) for compounds **1** and **2**

1	Ru–N (N-HSB)	Average Ru–N (bpy)
	2.069(7) and 2.064(8)	2.051(9)
2	Ru–N (N- $\frac{1}{2}$ HSB)	Average Ru–N (bpy)
	2.07(2) and 2.10(2)	2.06(2)

School of Chemistry, Trinity College Dublin, Dublin 2, Ireland.
E-mail: smdraper@tcd.ie

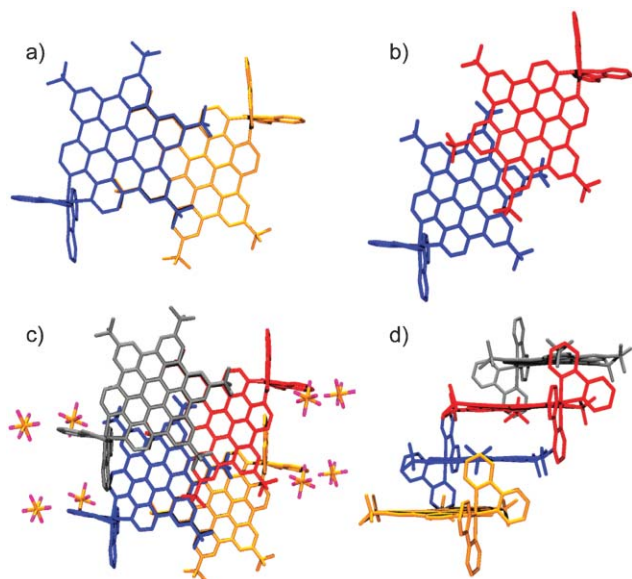


Fig. 2 Molecular packing of **1** showing, a) the eclipsed and b) the staggered overlap of two molecules; c) and d) show perpendicular views of the same four molecules of **1** in an off-set columnar stack. The PF_6^- anions have been removed for clarity from each image except c), where the eight sites of four partially occupied PF_6^- anions are shown.

columnar stack in the crystal (Fig. 2). The lean of this stack from the perpendicular is $\sim 40^\circ$. The stacking involves the eclipsed overlap of the 12 aromatic carbon atoms of rings 2 and 3 (Fig. 2a and Fig. 1 for ring labeling) and the staggered overlap of 8 carbon atoms in rings 3 and 4 (Fig. 2b). In both interactions the steric bulk of the peripheral *tert*-butyl groups is thought to be responsible for the large inter-planar spacing (distance between the mean planes of eclipsed and staggered molecules, 4.26(2) Å and 4.29(2) Å, respectively) and to inhibit any further overlap of adjacent molecules.

Interestingly, the *tert*-butyl groups of rings 3, 4 and 5 orient in the same direction and this is opposite to that of ring 2. They are positioned so that the axial methyl of each *tert*-butyl on rings 3 and 4 is rotated away from a second staggered molecule of **1** and so that the axial methyl of the *tert*-butyl group on ring 2 is oriented away from a second eclipsed molecule of **1**. In this way the steric interactions resulting from the staggered and eclipsed overlap of each molecule are minimised, allowing a degree of sideways lateral freedom. Ring 3 is involved in both stacking interactions and its *tert*-butyl group appears to be additionally influenced by a fully occupied PF_6^- anion. Of the two PF_6^- anions per molecule, that with full occupancy is nestled in the step formed between two neighbouring molecules (Fig. 3). The other anion, delocalised over two sites (50% occupancy each), is located on the outskirts of the bpy-flanked edges of the stack (Fig. 2c).

Fueled by the observation of dimers separated by solvent molecules in the solid state structures or Ru^{II} eilatins, it was suggested previously that the steric influence of the bpy ligands would direct the formation of discrete dimers rather than higher aggregates in **1**. However, the increase in size of the planar, ring-fused section of N-HSB compared to eilatin relieves the steric interaction of the bpy ligands, allowing for more extensive aggregation than first proposed (Fig. 2d), resulting in off-set stacks of N-HSB disks. N-HSB is clearly a ligand of novel dimensions.

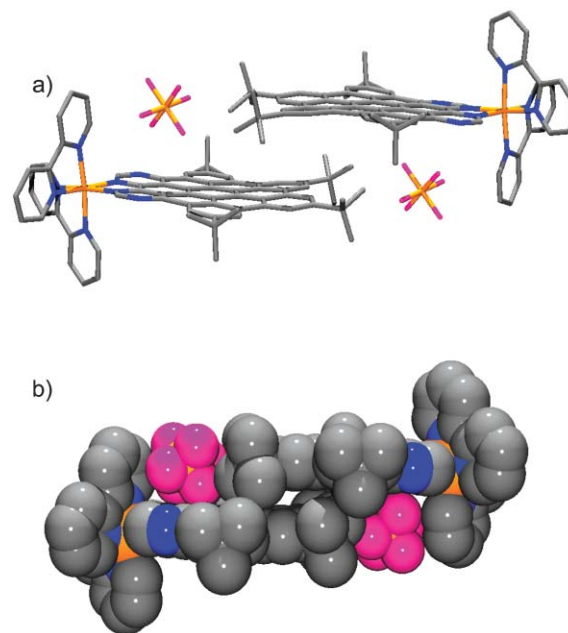


Fig. 3 a) Wire-frame and b) space-filling representations showing the staggered overlap of two molecules of **1** and the fully occupied PF_6^- anions nestled in-between.

In contrast to highly planar **1**, the saddle-like structure of **2** is exceedingly distorted (Fig. 4). The partially cyclised N- $\frac{1}{2}$ HSB ligand possesses two free phenyl rings which not only twist, but bow out from the fused portion of the ligand ($\sim 20^\circ$). The distortion from planarity in the fused ring portion of **2** is also considerable ($\sim 5^\circ$).§ Not only does **2** have a unique motif, but the distortion it exhibits is unprecedented in a metal coordination complex. Where observed before such distortion has been reserved for fused-ring polyaromatics.¹⁴ The curvature of the saddle-like structure of the N- $\frac{1}{2}$ HSB ligand is the result of minimising phenyl-phenyl interactions and enhancing electron delocalisation and ensures that in contrast to **1**, face-to-face π -stacking interactions between adjacent units are restricted.

Poor crystal quality and consequent refinement preclude detailed discussion of the structure, but packing in the solid-state reveals a “back-to-back” bimolecular arrangement leaving a solvent accessible void between the undersides of the saddles. No solvent could be located in this void (Fig. 4b).¶ The best resolved hexafluorophosphate counterion of each molecule of **2** is cradled in the seat of each saddle, leaving the remaining PF_6^- located on the periphery of the framework.

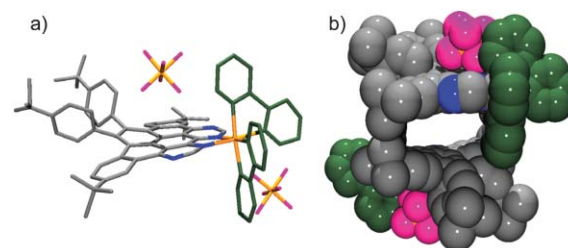


Fig. 4 a) A wire-frame representation of **2** illustrating its saddle-like nature and cradled PF_6^- anion and b) the space filling representation of two molecules of **2** showing the solvent accessible void.

In conclusion we have described the molecular structures of the ruthenium complexes $[\text{Ru}(\text{bpy})_2(\text{N-HSB})]\cdot 2\text{PF}_6$ and $[\text{Ru}(\text{bpy})_2(\text{N}-\frac{1}{2}\text{HSB})]\cdot 2\text{PF}_6$. The highly planar N-HSB ligand provides an aromatic platform for the self-assembly of $[\text{Ru}(\text{bpy})_2(\text{N-HSB})]\cdot 2\text{PF}_6$ into an off-set columnar stack. The free phenyl rings cause distortion in the partially cyclised N- $\frac{1}{2}$ HSB reducing the planarity and producing the saddle-like molecular structure of $[\text{Ru}(\text{bpy})_2(\text{N}-\frac{1}{2}\text{HSB})]\cdot 2\text{PF}_6$. The solid-state structural analyses of **1** and **2** reinforce and refine the conclusions made previously with regard to molecular interactions in solution. In addition they shed new light on the extent to which ligand size and design is influential in the formation of supramolecular aggregates. Such information is fundamental to the development and application of metal based nano-materials.

Notes and references

† Crystal data for **1**: $\text{C}_{74}\text{H}_{62}\text{N}_8\text{F}_{12}\text{P}_2\text{Ru}$, $M = 1454.33$, triclinic, space group $P-1$, $a = 11.6396(12)$, $b = 16.9812(17)$, $c = 18.4297(18)$ Å, $\alpha = 87.348(4)$, $\beta = 73.266(4)$, $\gamma = 84.678(4)^\circ$, $V = 3472.7(6)$ Å³, $Z = 2$, $D_c = 1.391$ Mg m⁻³, $\mu = 0.353$ mm⁻¹, $F(000) = 1488$, red lath $0.34 \times 0.04 \times 0.01$ mm, $2\theta_{\text{max}} = 42.16^\circ$, synchrotron ($\lambda = 0.68870$ Å), $T = 150(2)$ K, $T_{\text{max}} = 0.997$, $T_{\text{min}} = 0.600$, 19499 reflections, 8218 unique (99.0% completeness), 937 parameters, $wR_2 = 0.2759$ for all data, for 4916 data with $I > 2\sigma(I)$. One of the two hexafluorophosphate anions is disordered over two sites with 50% occupancy of each. CCDC 291925 (**1**). For crystallographic data in CIF or other electronic format see DOI: 10.1039/b604131k

‡ Crystal data for **2**: $\text{C}_{74}\text{H}_{68}\text{N}_8\text{F}_{12}\text{P}_2\text{Ru}$, $M = 1460.37$, triclinic, space group $P-1$, $a = 13.277(2)$, $b = 17.707(2)$, $c = 18.273(2)$ Å, $\alpha = 68.345(2)$, $\beta = 89.786(2)$, $\gamma = 78.094(2)^\circ$, $V = 3894.4(8)$ Å³, $Z = 2$, $D_c = 1.245$ Mg m⁻³, $\mu = 0.315$ mm⁻¹, $F(000) = 1500$, orange plate $0.12 \times 0.11 \times 0.01$ mm, $2\theta_{\text{max}} = 39.72^\circ$, synchrotron radiation ($\lambda = 0.67780$ Å), $T = 150(2)$ K, $T_{\text{max}} = 0.997$, $T_{\text{min}} = 0.598$, 19935 reflections, 8129 unique (98.8% completeness), 876 parameters, $wR_2 = 0.5001$ for all data, $R_1 = 0.1962$ for 4839 data with $I > 2\sigma(I)$. CCDC 291926 (**2**). For crystallographic data in CIF or other electronic format see DOI: 10.1039/b604131k. Numerous attempts were made to collect diffraction intensity data from hard won single crystal samples of **1** and **2** using a Bruker APEX diffractometer with MoK α radiation source. Samples were submitted to Station 9.8 of the SRS at Daresbury Laboratories, and data collected using a Bruker Nonius APEX II CCD diffractometer equipped and cooled by a Cryostream nitrogen-gas stream. Lorentz, polarisation and multi-scan absorption corrections were applied. The structures were solved using direct methods (SHELXS) and a full-matrix least-squares refinement performed on F^2 using all data (SHELXL97). Despite the use of high intensity synchrotron radiation, the two sets of crystals proved weakly diffracting. Both contain solvent accessible voids, however, no electron density peaks were found in

chemically sensible positions for solvent molecules. This work was supported by Enterprise Ireland award IF-2001\369 and IRCSET PD 02101. We acknowledge the provision of time on the Small Molecule Crystallography Service at the CCLRC Daresbury Laboratory via the E.U. FP6 "Structuring the European Research Area" Programme (through the Integrated Infrastructure Initiative "Integrating Activity on Synchrotron and Free Electron Laser Science").

§ Average angle calculated using the mean-plane of ring 8, the centroid of ring 8 and the carbon atoms of the free phenyl rings attached to the *tert*-butyl groups. Carbon atoms at the periphery of the fused system; average distortions of ~ 0.5 Å above and below the mean-plane.

¶ Treatment of the structure with the squeeze algorithm significantly reduced the R-factor ($R_1(\text{sqz}) = 0.1680$ ($I > 2\sigma$), $wR_2(\text{sqz}) = 0.4460$ (all data)).¹⁶

- G. R. Desiraju, *Chem. Commun.*, 2005, 2995; T. Steiner, *Angew. Chem., Int. Ed.*, 2002, **41**, 48.
- J. P. Hill, W. Jin, A. Kosaka, T. Fukushima, H. Ichihara, T. Shimomura, K. Ito, T. Hashizume, N. Ishii and T. Aida, *Science*, 2004, **304**, 1481.
- M. W. Hosseini, *Coord. Chem. Rev.*, 2003, **240**, 157.
- C. A. Hunter and J. K. M. Sanders, *J. Am. Chem. Soc.*, 1990, **112**, 5525; C. A. Hunter, K. R. Lawson, J. Perkins and C. J. Urch, *J. Chem. Soc., Perkin Trans. 2*, 2001, 651; C. Janiak, *J. Chem. Soc., Dalton Trans.*, 2000, 3885.
- A. Fechtenkotter, K. Saalwachter, M. A. Harbison, K. Müllen and H. W. Spiess, *Angew. Chem., Int. Ed.*, 1999, **38**, 3039.
- J. Wu, A. Fechtenkotter, J. Gauss, D. Watson Mark, M. Kastler, C. Fechtenkotter, M. Wagner and K. Müllen, *J. Am. Chem. Soc.*, 2004, **126**, 11311.
- S. M. Draper, D. J. Gregg and R. Madathil, *J. Am. Chem. Soc.*, 2002, **124**, 3486; D. J. Gregg, C. M. A. Ollagnier, C. M. Fitchett and S. M. Draper, *Chem.-Eur. J.*, 2006, DOI: 10.1002/chem.200501289.
- D. Gut, A. Rudi, J. Kopilov, I. Goldberg and M. Kol, *J. Am. Chem. Soc.*, 2002, **124**, 5449.
- S. D. Bergman, D. Reshef, L. Frish, Y. Cohen, I. Goldberg and M. Kol, *Inorg. Chem.*, 2004, **43**, 3792.
- S. D. Bergman, D. Reshef, S. Groysman, I. Goldberg and M. Kol, *Chem. Commun.*, 2002, 2374.
- S. M. Draper, D. J. Gregg, E. R. Schofield, W. R. Browne, M. Duati, J. G. Vos and P. Passaniti, *J. Am. Chem. Soc.*, 2004, **126**, 8694.
- D. J. Gregg, E. Bothe, P. Höfer, P. Passaniti and S. M. Draper, *Inorg. Chem.*, 2005, **44**, 5654.
- W. Zhaohui, Z. Tomovic, M. Kastler, R. Pretsch, F. Negri, V. Enkelmann and K. Müllen, *J. Am. Chem. Soc.*, 2004, **126**, 7794.
- J. Lu, J. Zhang, X. Shen, D. M. Ho and R. A. Pascal, Jr., *J. Am. Chem. Soc.*, 2002, **124**, 8035.
- R. J. Cernik, W. Clegg, C. R. A. Catlow, G. Bushnell-Wye, J. V. Flaherty, G. N. Greaves, I. Burrows, D. J. Taylor, S. J. Teat and M. Hamichi, *J. Synchrotron Radiat.*, 1997, **4**, 279.
- P. van der Silins and A. L. Spek, *Acta Crystallogr., Sect. A.*, 1990, **A46**, 194.